Soil Dynamics and Earthquake Engineering 143 (2021) 106605

Contents lists available at ScienceDirect

Soil Dynamics and Earthquake Engineering

journal homepage: http://www.elsevier.com/locate/soildyn

A general frequency adaptive framework for damped response analysis of wind turbines

S. Adhikari [a], S. Bhattacharya [b,*]

[a] College of Engineering, Swansea University, Swansea, UK
[b] Department of Civil and Environmental Engineering, University of Surrey, Guildford, Surrey, UK

ARTICLE INFO

Keywords:
Wind turbine
Dynamic response
Damping
Foundation stiffness
Harmonic excitation
Offshore

ABSTRACT

Dynamic response analysis of wind turbine towers plays a pivotal role in their analysis, design, stability, performance and safety. Despite extensive research, the quantification of general dynamic response remains challenging due to an inherent lack of the ability to model and incorporate damping from a physical standpoint. This paper develops a frequency adaptive framework for the analysis of the dynamic response of wind turbines under general harmonic forcing with a damped and flexible foundation. The proposed method is founded on an augmented dynamic stiffness formulation based on a Euler-Bernoulli beam-column with elastic end supports along with tip mass and rotary inertia arising from the nacelle of the wind turbine. The dynamic stiffness coefficients are derived from the complex-valued transcendental displacement function which is the exact solution of the governing partial differential equation with appropriate boundary conditions. The closed-form analytical expressions of the dynamic response derived in the paper are exact and valid for higher frequency ranges. The proposed approach avoids the classical modal analysis and consequently the ad-hoc use of the modal damping factors are not necessary. It is shown that the damping in the wind turbine dynamic analysis is completely captured by seven different physically-realistic damping factors. Numerical results shown in the paper quantify the distinctive nature of the impact of the different damping factors. The exact closed-form analytical expressions derived in the paper can be used for benchmarking related experimental and finite element studies and at the initial design/analysis stage.

1. Introduction

The United Nations has recently declared that we are facing a grave climate emergency and some of the most common manifestations are continuous ocean and atmospheric warming, heat waves and rise in sea level. A practical way to combat climate change and to achieve net-zero emission target to run a country mostly on electricity produced from renewable sources without burning much fossil fuel. Offshore wind turbines have the proven potential for the island and coastal nations and as a result, there is a tremendous rise in the proportion of electricity generation from such sources.

Offshore Wind Turbines are being currently constructed around the world and in extremely challenging sites, see for example deeper water developments and using floating system (Hywind in Scotland, see Ref. [1]), the typhoon and hurricane sites in Japan and China, seismic locations in Taiwan, China, Korea and India [2]. These sites often apply dynamic loading to the structure and the magnitude depends on the location. Due to its shape and form, offshore wind turbine structures are dynamically sensitive as a large rotating mass is applied at the top of the long slender column. Furthermore, the natural frequency of these structures is also close to the forcing frequencies. The typical natural frequency of a 3.6 MW turbine is about 0.33 Hz and that of an 8 MW is 0.22 Hz. As the turbines get larger, the target natural frequency of the overall wind turbine system gets lower and comes near to the wave frequencies. In some offshore development, predicting dynamic responses becomes the main challenge. For example, the predominant wave period in Yellow sea and Bohai sea (Chinese waters) is about 4.8–5 sec [3] and wave loading becomes a critical design consideration for turbines above 8 MW. There are other considerations such as corrosion and fatigue [4] and scour [5]. The readers are referred to studies on dynamics of offshore wind turbine by Zuo et al. [6], Sellami et al. [7], Banerjee at al [8] and Sclavounos et al. [9].

Guided by Limit State philosophy, a design must satisfy the following limit states: ULS (Ultimate Limit State), SLS (Serviceability Limit State),

* Corresponding author.
E-mail addresses: S.Adhikari@swansea.ac.uk (S. Adhikari), s.bhattacharya@surrey.ac.uk (S. Bhattacharya).

https://doi.org/10.1016/j.soildyn.2021.106605
Received 11 August 2020; Received in revised form 16 January 2021; Accepted 18 January 2021

FLS (Fatigue Limit State) and ALS (Accidental Limit State). To evaluate any of the above limit states for different dynamic load scenarios, the response of the structure must be evaluated. A quick method of evaluation of dynamic helps to optimize the design of a given turbine (for a given RNA mass and 1P frequency range) at a given site (wind field and wave/sea states) through the change in physical parameters i.e. foundation stiffness and tower stiffness. In certain challenging sites where the forcing frequency is very close to the natural frequency, damping plays a beneficial role in optimization. There are different sources of damping in an offshore wind turbine: Aerodynamic, hydrodynamic, structural damping, material damping (including the soil). Recently several authors have considered explicit dynamic analysis of wind turbine structures. Bending, axial and torsional vibrations of wind turbines has been considered by Wang et al. [10] and Vitor Chaves et al. [11]. Due to the interest of understanding the performance of offshore wind turbines in seismic areas, dynamic analysis work is being conducted by He et al. [12], Patra and Haldar [13], Zhao M et al. [14] and Jiang W et al. [15]. These studies clearly demonstrate the need for comprehensive dynamic analysis of wind turbine structures.

It has also been established that Soil-Structure Interaction (SSI) is very important for predicting the short term and long-term performance of these structures. For design purposes SSI can be classified as follows: (1) Load transfer mechanism from the foundation to the soil (2) Modes of vibration of the whole system (3) Long term performance in the sense whether or not the foundation will tilt progressively under the combined action of millions of cycles of loads arising from the wind, wave and 1P (rotor frequency) and 2P/3P (blade passing frequency). In a series of previous studies, the authors [16–19] considered the analysis of the first natural frequency of wind turbines taking SSI into account. The recent trend in wind turbine design is towards very large systems. While such large systems give more power output, a potential disadvantage is that they can be susceptible to dynamic loads as the natural frequencies become lower. As a result, many resonance frequencies of the structure will be excited within the operating frequency ranges. Therefore, for a credible dynamic analysis, it is necessary to have a simple approach which can take account of multiple natural frequencies and vibration modes.

It is certainly possible to perform a classical modal analysis [20] for high-frequency vibration problems. However, there are two major issues. Firstly, analytical solutions for the natural frequencies and mode shapes are generally difficult to obtain beyond the first mode. Secondly, simplified proportional modal damping assumptions must be employed for the response analysis. One way these issues can be avoided is by using the dynamic stiffness method [21–25]. This approach can be considered within the broad class of spectral methods [26] for linear dynamical systems. A key feature of the dynamic stiffness method is the use of complex shape functions (due to the presence of damping) which are frequency-dependent [27]. The mass distribution of the element is treated exactly in deriving the element dynamic stiffness matrix. The method does not employ eigenfunction expansions and, consequently, a major step of the traditional finite element analysis, namely, the determination of natural frequencies and mode shapes, is eliminated which automatically avoids the errors due to series truncation [28]. Since the modal expansion is not employed, ad hoc assumptions concerning the damping matrix being proportional to the mass and/or stiffness are not necessary. The dynamic stiffness matrix of one-dimensional structural elements, taking into account the effects of flexure, torsion, axial and shear deformation, and damping, is exactly determinable, which, in turn, enables the exact vibration analysis by an inversion of the global dynamic stiffness matrix [22]. The method is essentially a frequency-domain approach suitable for steady-state harmonic or stationary random excitation problems. The static stiffness matrix and the consistent mass matrix appear as the first two terms in the Taylor expansion [21,29] of the dynamic stiffness matrix in the frequency parameter.

The overview of the paper is as follows. In Section 2 an overview of dynamic stiffness of undamped beam-columns is given. In particular, the equation of motion is discussed in Subsection 2.1, the characteristic equation and essential non-dimensional parameters are explained in Subsection 2.2 and the undamped dynamic stiffness matrix is derived in Subsection 2.3. The dynamic stiffness matrix for damped beam-columns are derived in Section 3. The effect of end restraints and tip mass in considered in Section 4. The consideration of tip mass and rotary inertia in discussed in Subsection 4.1, while the consideration of damped and flexible foundation is proposed in Subsection 4.2. The analysis of dynamic response in the frequency domain is developed in Section 5 where exact closed-form expressions have been derived for systems with fixed foundation (Subsection 5.1) and systems with damped and flexible foundation (Subsection 5.2). The new expressions derived in the paper is summarised in Section 6 and main conclusions are drawn in Section 7.

2. Overview of dynamic stiffness of undamped beam-columns

In Fig. 1, the schematic diagram of wind turbine tower constrained by flexible springs is shown.

An Euler-Bernoulli beam model is used to mathematically represent the dynamics of the beam. The bending stiffness of the beam is EI and the beam is attached to the foundation. Here x is the spatial coordinate, starting at the bottom and moving along the height of the structure. The interaction of the structure with the foundation is modelled using two springs. The rotational spring with spring stiffness k_r, the lateral spring with spring stiffness k_l and the coupling spring with spring stiffness k_{lr} constrains the system at the bottom ($x = 0$). The beam has a top mass with rotary inertia J and mass M. This top mass is used to idealise the rotor and blade system. The mass per unit length of the beam is m and the beam is subjected to a constant compressive axial load $P = Mg$. Although the motivation of this study is arising from the large offshore wind turbines, the analytical formulation proposed here is not restricted to offshore wind turbines. With suitable values of k_r, k_l and k_{lr}, this analysis can be applied on onshore wind turbines also.

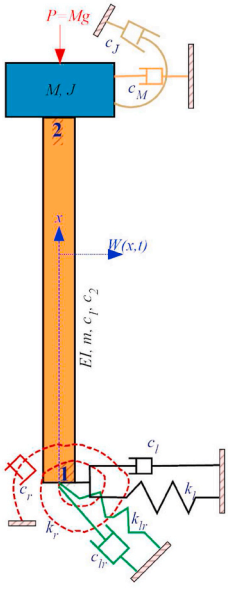

Fig. 1. A damped Euler Bernoulli beam with a top mass and point dampers are employed for dynamic analysis of a wind turbine tower. Dynamic foundation-structure interaction is modelled by three flexible springs and dampers. The mass of the blades and the rotor-hub are assumed to be M. The damping parameters c_M and c_J denote aerodynamic damping corresponding to linear and rotary motion of the top mass (nacelle). c_1 is the strain-rate-dependent viscous damping coefficient and c_2 is the velocity-dependent viscous damping coefficient of the wind turbine tower. c_r, c_l and c_{lr} correspond to rotational, lateral and coupling damping coefficients of the foundation.

2.1. Equation of motion

The fourth-order partial differential equation describing the equation of motion of a Euler Bernoulli beam (see for example [20,30,31]) is given by

$$EI\frac{\partial^4 W(x,t)}{\partial x^4}+P\frac{\partial^2 W(x,t)}{\partial x^2}+m\,\ddot{W}(x,t)=F(x,t) \tag{1}$$

Here $W(x,t)$ is the transverse deflection of the beam, t is time, $(\dot{\bullet})$ denotes derivative with respect to time and $F(x,t)$ is the applied time depended load on the beam. The height of the structure is considered to be L. Our central aim is to obtain the dynamic response in the frequency domain *without* calculating the natural frequencies of the system. Here we develop an approach based on the non-dimensionalisation of the equation of motion (1) in conjunction with the dynamic stiffness method.

2.2. Characteristic equation and non-dimensional parameters

In previous works [16–19] the authors developed a method for the calculation of the natural frequencies of system (1) based on the non-dimensionalisation of the equation of motion and the boundary conditions. A complete different strategy is adopted here. The aim is to express the dynamics of the beam by a finite-element like discretised system. However, unlike the conventional finite element method where frequency-independent cubic polynomial is used for discretisation, we aim to use functions which ere the exact solutions of the dynamic system. This functions arise from the characteristic equation as discussed below.

We consider free vibration so that the forcing can be assumed to be zero. Assuming harmonic solution we have

$$W(x,t)=w(\xi)\exp\{\mathrm{i}\omega t\} \tag{2}$$

where $\mathrm{i}=\sqrt{-1}$, ω is the excitation frequency and the normalised length

$$\xi=x/L \tag{3}$$

Substituting this in the equation of motion one has

$$\frac{EI}{L^4}\frac{\mathrm{d}^4 w(\xi)}{\mathrm{d}\xi^4}+\frac{P}{L^2}\frac{\mathrm{d}^2 w(\xi)}{\mathrm{d}\xi^2}-m\omega^2 w(\xi)=0 \tag{4}$$

$$\text{or}\quad \frac{\mathrm{d}^4 w(\xi)}{\mathrm{d}\xi^4}+\nu\frac{\mathrm{d}^2 w(\xi)}{\mathrm{d}\xi^2}-\Omega^2 w(\xi)=0 \tag{5}$$

Here the non-dimensional parameters can be identified as

$$\begin{aligned}&\nu=\frac{PL^2}{EI}\quad \text{(nondimensional axial force)}\\ &\Omega^2=\omega^2\frac{mL^4}{EI}=\omega^2c^2\quad \text{(nondimensional frequency parameter)}\\ &\text{where}\quad c^2=\frac{mL^4}{EI}\quad \text{(frequency scaling parameter)}\end{aligned} \tag{6}$$

The effect of rotary inertia is ignored in the above formulation. If this effect is to be included, then ν should be replaced by Refs. [16,18] by $\widetilde{\nu}$ defined as

$$\widetilde{\nu}=\nu+\mu^2\Omega^2 \tag{7}$$

where

$$\mu=\frac{r}{L}\quad \text{(nondimensional radius of gyration)} \tag{8}$$

Assuming a solution of the form

$$w(\xi)=\exp\{\lambda\xi\} \tag{9}$$

and substituting in the equation of motion (4) results

$$\lambda^4+\nu\lambda^2-\Omega^2=0 \tag{10}$$

This equation is often known as the dispersion relationship. This is the equation which underpins the dynamic shape functions of the beam. Solving this equation for λ^2 we have

$$\begin{aligned}\lambda^2&=-\frac{\nu}{2}\pm\sqrt{\left(\frac{\nu}{2}\right)^2+\Omega^2}\\ &=-\left(\underbrace{\sqrt{\left(\frac{\nu}{2}\right)^2+\Omega^2}+\frac{\nu}{2}}_{\lambda_1^2}\right),\quad \left(\underbrace{\sqrt{\left(\frac{\nu}{2}\right)^2+\Omega^2}-\frac{\nu}{2}}_{\lambda_2^2}\right)\end{aligned} \tag{11}$$

Because ν^2 and Ω^2 are always positive quantities, both roots are real with one negative and one positive root. Therefore, the four roots can be expressed as

$$\lambda=\pm\,\mathrm{i}\lambda_1,\quad \pm\lambda_2 \tag{12}$$

where

$$\lambda_1=\left(\sqrt{\left(\frac{\nu}{2}\right)^2+\Omega^2}+\frac{\nu}{2}\right)^{1/2}\geq 0 \tag{13}$$

$$\text{and}\quad \lambda_2=\left(\sqrt{\left(\frac{\nu}{2}\right)^2+\Omega^2}-\frac{\nu}{2}\right)^{1/2}\geq 0 \tag{14}$$

In view of the roots in equation (12), the solution $w(\xi)$ can be expressed as

$$\begin{aligned}&w(\xi)=w_1\sin\lambda_1\xi+w_2\cos\lambda_1\xi+w_3\sinh\lambda_2\xi+w_4\cosh\lambda_2\xi\\ &\text{or}\quad w(\xi)=\mathbf{s}^T(\xi)\mathbf{w}\end{aligned} \tag{15}$$

where the vectors

$$\mathbf{s}(\xi,\omega)=\{\cos\lambda_1\xi,\ \sin\lambda_1\xi,\ \cosh\lambda_2\xi,\ \sinh\lambda_2\xi\}^T \tag{16}$$

$$\text{and}\quad \mathbf{w}=\{w_1,w_2,w_3,w_4\}^T \tag{17}$$

Next we use these solutions to obtain the dynamic shape functions of the beam.

2.3. Undamped dynamic stiffness matrix

2.3.1. Frequency dependent shape functions

For classical (static) finite element analysis of beams, cubic polynomials are used as shape functions (see for example [32]). Here we aim to incorporate frequency dependent dynamic shape functions, as used with the framework of the dynamic finite element method. The dynamic shape functions are obtained such that the equation of dynamic equilibrium is satisfied exactly at all points within the element. Similar to the classical finite element method, assume that the frequency-dependent displacement within an element is interpolated from the nodal displacements as

$$w(\xi,\omega)=\mathbf{N}^T(\xi,\omega)\mathbf{w}(\omega) \tag{18}$$

Here $\mathbf{w}(\omega)\in\mathrm{R}^n$ is the nodal displacement vector $\mathbf{N}(\xi,\omega)\in\mathrm{R}^n$ is the vector of frequency-dependent shape functions and $n=4$ is the number of the nodal degrees-of-freedom. Using the vector of the basis functions $\mathbf{s}(\xi,\omega)$ in Eq. (16), the shape function vector can be expressed as

$$\mathbf{N}^T(\xi,\omega)=\mathbf{s}^T(\xi,\omega)\mathbf{\Gamma}(\omega) \tag{19}$$

The matrix $\mathbf{\Gamma}(\omega)\in\mathrm{C}^{4\times 4}$ depends on the boundary conditions. An element for the damped beam under bending vibration is shown in Fig. 2.

The relationship between the shape functions and the boundary conditions can be represented as in Table 1, where boundary conditions in each column give rise to the corresponding shape function.

Writing Eq. (18) for the above four sets of boundary conditions, one

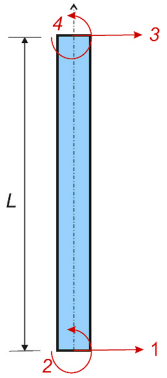

Fig. 2. A dynamic element for the bending vibration of a beam. It has two nodes and four degrees of freedom. The displacement field within the element is expressed by frequency dependent shape functions.

Table 1
The four different boundary conditions used to derive the dynamic shape functions of the beam.

	$N_1(\xi,\omega)$	$N_2(\xi,\omega)$	$N_3(\xi,\omega)$	$N_4(\xi,\omega)$
$w(0,\omega)$	1	0	0	0
$\frac{dw(\xi,\omega)}{d\xi}\|_{\xi=0}$	0	1	0	0
$w(1,\omega)$	0	0	1	0
$\frac{dw(\xi,\omega)}{d\xi}\|_{\xi=1}$	0	0	0	1

obtains

$$[\mathbf{R}][\widehat{\mathbf{w}}^{(1)},\widehat{\mathbf{w}}^{(2)},\widehat{\mathbf{w}}^{(3)},\widehat{\mathbf{w}}^{(4)}]=\mathbf{I} \tag{20}$$

where (omitting ω for convienece)

$$\mathbf{R}=\begin{bmatrix} s_1(0) & s_2(0) & s_3(0) & s_4(0) \\ \frac{ds_1}{d\xi}(0) & \frac{ds_2}{d\xi}(0) & \frac{ds_3}{d\xi}(0) & \frac{ds_4}{d\xi}(0) \\ s_1(1) & s_2(1) & s_3(1) & s_4(1) \\ \frac{ds_1}{d\xi}(1) & \frac{ds_2}{d\xi}(1) & \frac{ds_3}{d\xi}(1) & \frac{ds_4}{d\xi}(1) \end{bmatrix} = \begin{bmatrix} 1 & 0 & 1 & 0 \\ 0 & \lambda_1 & 0 & \lambda_2 \\ \cos(\lambda_1) & \sin(\lambda_1) & \cosh(\lambda_2) & \sinh(\lambda_2) \\ -\sin(\lambda_1)\lambda_1 & \cos(\lambda_1)\lambda_1 & \sinh(\lambda_2)\lambda_2 & \cosh(\lambda_2)\lambda_2 \end{bmatrix} \tag{21}$$

and $\widehat{\mathbf{w}}^{(k)}$ is the vector of constants giving rise to the k-th shape function. In view of the boundary conditions represented in Table 1 and equation (20), the shape functions for bending vibration can be shown to be given by Eq. (19) where

Following [22] the functions $\Gamma_j, j=1,2,\cdots 6$ can be defined as

$$\begin{aligned}
\Gamma_1 &= (\lambda_2\sin(\lambda_1)-\lambda_1\sinh(\lambda_2))\left(\lambda_1^2+\lambda_2^2\right)/\Delta \\
\Gamma_2 &= (\lambda_1\cos(\lambda_1)\sinh(\lambda_2)-\lambda_2\sin(\lambda_1)\cosh(\lambda_2))\left(\lambda_1^2+\lambda_2^2\right)/\Delta \\
\Gamma_3 &= (\cos(\lambda_1)-\cosh(\lambda_2))\lambda_1\,\lambda_2\,\left(\lambda_1^2+\lambda_2^2\right)/\Delta \\
\Gamma_4 &= \left(\left(\lambda_1^2-\lambda_2^2\right)(1-\cos(\lambda_1)\cosh(\lambda_2))+2\,\lambda_1\,\lambda_2\sin(\lambda_1)\sinh(\lambda_2)\right)\lambda_1\,\lambda_2/\Delta \\
\Gamma_5 &= (\lambda_2\sinh(\lambda_2)+\lambda_1\sin(\lambda_1))\lambda_1\,\lambda_2\,\left(\lambda_1^2+\lambda_2^2\right)/\Delta \\
\Gamma_6 &= -(\lambda_1\cosh(\lambda_2)\sin(\lambda_1)+\lambda_2\sinh(\lambda_2)\cos(\lambda_1))\lambda_1\,\lambda_2\,\left(\lambda_1^2+\lambda_2^2\right)/\Delta
\end{aligned} \tag{23}$$

Here Δ, related to the determinant of the matrix $\mathbf{R}$, is given by

$$\Delta=-\det(\mathbf{R})=2\,\lambda_1\,\lambda_2\,(\cos(\lambda_1)\cosh(\lambda_2)-1)+\left(\lambda_1^2-\lambda_2^2\right)\sin(\lambda_1)\sinh(\lambda_2) \tag{24}$$

The above equations completely defines the shape function. Next we use them to obtain the dynamic stiffness matrix.

2.3.2. *Element dynamic stiffness matrix and the forcing vector*

The stiffness and mass matrices can be obtained following the conventional variational formulation [33]. The only difference is instead of classical cubic polynomials as the shape functions, frequency dependent shape functions in (19) should be used. The dynamic stiffness matrix is defined as

$$\mathbf{D}(\omega)=\mathbf{K}(\omega)-\mathbf{G}(\omega)-\omega^2\mathbf{M}(\omega) \tag{25}$$

so that the equation of dynamic equilibrium of the element is given be

$$\mathbf{D}(\omega)\mathbf{w}(\omega)=\mathbf{f}(\omega) \tag{26}$$

Here $\mathbf{f}(\omega)$ element forcing vector and the response vector $\mathbf{w}(\omega)$ is given by

$$\mathbf{w}(\omega)=\begin{Bmatrix} w_1(\omega) \\ w_2(\omega) \\ w_3(\omega) \\ w_4(\omega) \end{Bmatrix} = \begin{Bmatrix} \delta^{(1)}(\omega) \\ \theta^{(1)}(\omega) \\ \delta^{(2)}(\omega) \\ \theta^{(2)}(\omega) \end{Bmatrix} \tag{27}$$

Here $\delta^{(1)}(\omega),\theta^{(1)}(\omega)$ and $\delta^{(2)}(\omega),\theta^{(2)}(\omega)$ denotes the frequency dependent displacement and rotation at the bottom and top end of the wind-turbine tower respectively. In Eq. (25), the frequency-dependent stiffness, geometric stiffness and mass matrices can be obtained from

$$\mathbf{K}(\omega)=EI \times \int_0^L \frac{d^2\mathbf{N}(x/L,\omega)}{dx^2}\frac{d^2\mathbf{N}^T(x/L,\omega)}{dx^2}dx=\frac{EI}{L^3}\int_0^1 \frac{d^2\mathbf{N}(\xi,\omega)}{d\xi^2}\frac{d^2\mathbf{N}^T(\xi,\omega)}{d\xi^2}d\xi \tag{28}$$

$$\mathbf{G}(\omega)=P\int_0^L \frac{d\mathbf{N}(x/L,\omega)}{dx}\frac{d\mathbf{N}^T(x/L,\omega)}{dx}dx=PL\int_0^1 \frac{d\mathbf{N}(\xi,\omega)}{d\xi}\frac{d\mathbf{N}^T(\xi,\omega)}{d\xi}d\xi \tag{29}$$

$$\mathbf{\Gamma}(\omega)=[\widehat{\mathbf{w}}^{(1)},\widehat{\mathbf{w}}^{(2)},\widehat{\mathbf{w}}^{(3)},\widehat{\mathbf{w}}^{(4)}]=[\mathbf{R}^{-1}]=\frac{1}{\lambda_1^2+\lambda_2^2}\begin{bmatrix} \lambda_2^2-\Gamma_4 & \Gamma_2 L & -\Gamma_3 & \Gamma_1 L \\ -\frac{\Gamma_6}{\lambda_1} & \left(\lambda_1+\frac{\Gamma_4}{\lambda_1}\right)L^{-1} & -\frac{\Gamma_5}{\lambda_1} & -\frac{\Gamma_3 L}{\lambda_1} \\ \lambda_1^2+\Gamma_4 & -F_2 L & \Gamma_3 & -\Gamma_1 L \\ \frac{\Gamma_6}{\lambda_2} & \left(\lambda_2-\frac{\Gamma_4}{\lambda_2}\right)L^{-1} & \frac{\Gamma_5}{\lambda_2} & \frac{\Gamma_3 L}{\lambda_2} \end{bmatrix} \tag{22}$$

$$\text{and} \quad \mathbf{M}(\omega) = m\int_0^L \mathbf{N}(x/L,\omega)\mathbf{N}^T(x/L,\omega)\mathrm{d}x = mL\int_0^1 \mathbf{N}(\xi,\omega)\mathbf{N}^T(\xi,\omega)\mathrm{d}\xi \tag{30}$$

After some algebraic simplifications, it can be shown [22] that the dynamic stiffness matrix is given by the following closed-form expression

$$\mathbf{D}(\omega) = \frac{EI}{L^3}\begin{bmatrix} \Gamma_6 & -\Gamma_4 L & \Gamma_5 & \Gamma_3 L \\ -\Gamma_4 L & \Gamma_2 L^2 & -\Gamma_3 L & \Gamma_1 L^2 \\ \Gamma_5 & -\Gamma_3 L & \Gamma_6 & \Gamma_4 L \\ \Gamma_3 L & \Gamma_1 L^2 & \Gamma_4 L & \Gamma_2 L^2 \end{bmatrix} \tag{31}$$

The functions $\Gamma_j, j = 1, 2, \cdots 6$ are defined in (23). The elements of this matrix are frequency dependent quantities because λ_1 and λ_2 are functions of ω.

Considering the frequency representation of the forcing function in Eq. (1) we have

$$F(x,t) = f(\xi,\omega)\exp\{\mathrm{i}\omega t\} \tag{32}$$

where $f(\xi,\omega)$ is in general a spatially varying frequency dependent forcing function. Using this, the element forcing vector is defined as

$$\mathbf{f}(\omega) = \int_0^L f(x/L,\omega)\mathbf{N}(x/L,\omega)\mathrm{d}x = L\,\mathbf{\Gamma}^T(\omega)\int_0^1 f(\xi,\omega)\mathbf{s}(\xi,\omega)\mathrm{d}\xi \tag{33}$$

For a perfect harmonic excitation $f(\xi,\omega)$ is constant with respect the frequency. In addition, if the forcing is uniformly distributed over the length, then $f(\xi,\omega)$ is constant with respect to the non-dimension length parameter ξ also.

As dynamic stiffness is based on the exact solution of the governing differential equation, only one element is necessary to represent the entire beam for all frequency values. Therefore the 4 matrix equation in (26) described the exact dynamic of the wind turbine tower for any excitation frequency. So far damping in the system has not bee considered. Without the consideration of damping, Eq. (26) becomes singular for certain frequencies and therefore cannot be numerically used for all frequency values. In the next section we include damping effects in the equation of motion.

3. Dynamic stiffness of damped beam-columns

3.1. Systems with general damping

The equation of motion of a damped beam-column can be expressed as

$$EI\frac{\partial^4 W(x,t)}{\partial x^4} + c_1\frac{\partial^5 W(x,t)}{\partial x^4 \partial t} + P\frac{\partial^2 W(x,t)}{\partial x^2} + c_2\frac{\partial W(x,t)}{\partial t} + m\,\ddot{W}(x,t) = F(x,t) \tag{34}$$

It is assumed that the behaviour of the beam follows the Euler-Bernoulli hypotheses as before. In the above equation c_1 is the strain-rate-dependent viscous damping coefficient and c_2 is the velocity-dependent viscous damping coefficient. Considering harmonic motion with frequency ω as in Eq. (2) we have

$$\frac{EI}{L^4}\frac{\mathrm{d}^4 w(\xi)}{\mathrm{d}\xi^4} + \mathrm{i}\omega\frac{c_1}{L^4}\frac{\mathrm{d}^4 w(\xi)}{\mathrm{d}\xi^4} + \frac{P}{L^2}\frac{\mathrm{d}^2 w(\xi)}{\mathrm{d}\xi^2} + \mathrm{i}\omega c_2 w(\xi) - m\omega^2 w(\xi) = 0 \tag{35}$$

$$\text{or}\left(1 + \mathrm{i}\omega\frac{c_1}{EI}\right)\frac{\mathrm{d}^4 w(\xi)}{\mathrm{d}\xi^4} + \nu\frac{\mathrm{d}^2 w(\xi)}{\mathrm{d}\xi^2} - \Omega^2\left(1 - \mathrm{i}\frac{c_2}{m\omega}\right)w(\xi) = 0 \tag{36}$$

Following the damping convention in dynamic analysis as in Ref. [20], we consider stiffness and mass proportional damping. Therefore, we express the damping constants as

$$\frac{c_1}{EI} = \xi_1\sqrt{\frac{mL^4}{EI}} \quad \text{and} \quad \frac{c_2}{m} = \xi_2\Big/\sqrt{\frac{mL^4}{EI}} \tag{37}$$

where ξ_1 and ξ_2 are non-dimensional stiffness and mass proportional damping factors. Form the above expressions, these non-dimensional constants can be explicitly expressed in terms of the damping coefficients as

$$\xi_1 = \frac{c_1}{L^2\sqrt{m\,EI}} \quad (\text{strain} - \text{rate} - \text{dependent damping factor}) \tag{38}$$

$$\xi_2 = \frac{c_2 L^2}{\sqrt{m\,EI}} \quad (\text{velocity} - \text{dependent damping factor}) \tag{39}$$

Substituting these, Eq. (36) can be simplified as

$$(1 + \mathrm{i}\Omega\xi_1)\frac{\mathrm{d}^4 w(\xi)}{\mathrm{d}\xi^4} + \nu\frac{\mathrm{d}^2 w(\xi)}{\mathrm{d}\xi^2} - \Omega^2(1 - \mathrm{i}\xi_2/\Omega)w(\xi) = 0 \tag{40}$$

The characteristic equation therefore can be obtained as

$$(1 + \mathrm{i}\Omega\xi_1)\lambda^4 + \nu\lambda^2 - \Omega^2(1 - \mathrm{i}\xi_2/\Omega) = 0 \tag{41}$$

$$\text{or}\lambda^4 + \nu_d\lambda^2 - \Omega_d^2 = 0 \tag{42}$$

where

$$\nu_d = \frac{\nu}{1 + \mathrm{i}\Omega\xi_1} \tag{43}$$

$$\text{and} \quad \Omega_d^2 = \Omega^2\frac{(1 - \mathrm{i}\xi_2/\Omega)}{(1 + \mathrm{i}\Omega\xi_1)} \tag{44}$$

The dynamic stiffness matrix of the damped beam column can be obtained from the formulation derived in the previous section by replacing ν and Ω with ν_d and Ω_d respectively.

3.2. Special cases

We consider some familiar special cases to relate the general result in the previous section with know results.

3.2.1. Standard undamped beam without the axial force

For this case $\nu = 0$ and from equations (13) and (14) one obtains $\lambda_1 = \lambda_2 = \sqrt{\Omega} = \sqrt{\omega}\sqrt{\frac{mL^4}{EI}} = \bar{\lambda}$ (say). Substituting these in equation (31) and simplifying we obtain the dynamic stiffness matrix as

$$\mathbf{D}(\omega) = \frac{EI}{L^3}\begin{bmatrix} G_6 & -G_4 L & G_5 & G_3 L \\ -G_4 L & G_2 L^2 & -G_3 L & G_1 L^2 \\ G_5 & -G_3 L & G_6 & G_4 L \\ G_3 L & G_1 L^2 & G_4 L & G_2 L^2 \end{bmatrix} \tag{45}$$

where

$$G_1 = \frac{\bar{\lambda}\sin(\bar{\lambda}) - \bar{\lambda}\sinh(\bar{\lambda})}{\cos(\bar{\lambda})\cosh(\bar{\lambda}) - 1}, \quad G_2 = \frac{\bar{\lambda}\sinh(\bar{\lambda})\cos(\bar{\lambda}) - \bar{\lambda}\cosh(\bar{\lambda})\sin(\bar{\lambda})}{\cos(\bar{\lambda})\cosh(\bar{\lambda}) - 1}$$

$$G_3 = \frac{(\cos(\bar{\lambda}) - \cosh(\bar{\lambda}))\bar{\lambda}^2}{\cos(\bar{\lambda})\cosh(\bar{\lambda}) - 1}, \quad G_4 = \frac{\bar{\lambda}^2\sin(\bar{\lambda})\sinh(\bar{\lambda})}{\cos(\bar{\lambda})\cosh(\bar{\lambda}) - 1}$$

$$G_5 = \frac{(\bar{\lambda}\sinh(\bar{\lambda}) + \bar{\lambda}\sin(\bar{\lambda}))\bar{\lambda}^2}{\cos(\bar{\lambda})\cosh(\bar{\lambda}) - 1}, \quad G_6 = -\frac{(\bar{\lambda}\cosh(\bar{\lambda})\sin(\bar{\lambda}) + \bar{\lambda}\sinh(\bar{\lambda})\cos(\bar{\lambda}))\bar{\lambda}^2}{\cos(\bar{\lambda})\cosh(\bar{\lambda}) - 1} \tag{46}$$

The dynamic stiffness matrix in (45) matches exactly with the dynamic stiffness matrix of the Euler-Bernoulli beams as given in Ref. [21].

3.2.2. The static limit

When no axial force is present, the static limit is obtained by taking the mathematical limit of $\omega \to 0$. Using this limit in the expression of G_j, $j = 1, \cdots, 6$ in equation (46), from the expression of the dynamic stiffness matrix in (45) we have

$$\mathbf{K}_{EB} = \lim_{\omega \to 0} \mathbf{D}(\omega) = \frac{EI}{L^3} \begin{bmatrix} 12 & 6L & -12 & 6L \\ 6L & 4L^2 & -6L & 2L^2 \\ -12 & -6L & 12 & -6L \\ 6L & 2L^2 & -6L & 4L^2 \end{bmatrix} \tag{47}$$

This limiting matrix is exactly the same as the conventional stiffness matrix for Euler-Bernoulli beams [33]. Therefore, the dynamic stiffness matrix proposed here is a generalisation in the frequency domain.

4. Effect of end restraints and tip mass

4.1. The consideration of the top mass and rotary inertia

The mass of the nacelle and rotor blades are represented by M in Fig. 1. This is very significant and can be more than the mass of the tower. Due to non-negligible geometric dimension, this mass cannot be modelled as a classical point mass. Therefore, rotary inertia of this mass should also be taken into account. We assume that the rotary inertia of the top mass is given by J. From practical experiences it is known that the top mass is subjected to significant aerodynamic damping. Therefore, this must also be taken into account in an exact and effective manner. In order to incorporate the effect of M and J, together with their corresponding damping within the scope of the dynamic stiffness approach, we consider a zero-length damped 'finite element' corresponding to the degree of freedom of the top point (point 2 in Fig. 1). The dynamic equilibrium of this element can be expressed by the following matrix equation

$$\underbrace{\begin{bmatrix} -\omega^2 M + \mathrm{i}\omega c_M & 0 \\ 0 & -\omega^2 J + \mathrm{i}\omega c_J \end{bmatrix}}_{\mathbf{D}_2(\omega)} \begin{Bmatrix} w_3 \\ w_4 \end{Bmatrix} = \begin{Bmatrix} f_3 \\ f_4 \end{Bmatrix} \tag{48}$$

Here the damping constants c_M and c_J correspond to linear and rotational damping of the top mass. Following the notations of the degrees of freedom in 2, it should be noted that w_3 is the displacement and w_4 is the rotation of the top point. We introduce the two following non-dimensional parameters

$$\alpha = \frac{M}{mL} \quad (\text{non} - \text{dimensional mass ratio}) \tag{49}$$

$$\beta = \frac{J}{mL^3} \quad (\text{non} - \text{dimensional rotary inertia}) \tag{50}$$

Using these quantities it can be deduced that

$$\omega^2 M = \omega^2 \alpha m L = \Omega^2 \frac{EI}{mL^4} \alpha m L = \frac{EI}{L^3} \Omega^2 \alpha \tag{51}$$

$$\omega^2 J = \omega^2 \beta m L^3 = \Omega^2 \frac{EI}{mL^4} \beta m L^3 = \frac{EI}{L^3} \Omega^2 \beta L^2 \tag{52}$$

As a result the dynamic stiffness matrix corresponding to the top mass element becomes

$$\mathbf{D}_2(\omega) = \frac{EI}{L^3} \begin{bmatrix} -\Omega^2 \overline{\alpha} & 0 \\ 0 & -\Omega^2 \overline{\beta} L^2 \end{bmatrix} \tag{53}$$

In the above equation, the complex frequency-dependent quantities $\overline{\alpha}$ and $\overline{\beta}$ are defined as

$$\overline{\alpha} = \alpha - \mathrm{i}\frac{\xi_M}{\Omega} \quad (\text{damped non} - \text{dimensional mass ratio}) \tag{54}$$

$$\text{and} \quad \overline{\beta} = \beta - \mathrm{i}\frac{\xi_J}{\Omega} \quad (\text{damped non} - \text{dimensional rotary inertia}) \tag{55}$$

After some algebraic simplifications, the following new non-dimensional damping parameters are identified as

$$\xi_M = \frac{c_M L}{\sqrt{m\, EI}} \quad (\text{mass damping factor}) \tag{56}$$

$$\text{and} \quad \xi_J = \frac{c_J}{L\sqrt{m\, EI}} \quad (\text{rotary damping factor}) \tag{57}$$

Adding this with the dynamic stiffness matrix of the beam we have the effective stiffness matrix as

$$\mathbf{D}_e(\omega) = \frac{EI}{L^3} \begin{bmatrix} \Gamma_6 & -\Gamma_4 L & \Gamma_5 & \Gamma_3 L \\ -\Gamma_4 L & \Gamma_2 L^2 & -\Gamma_3 L & \Gamma_1 L^2 \\ \Gamma_5 & -\Gamma_3 L & (\Gamma_6 - \Omega^2 \overline{\alpha}) & \Gamma_4 L \\ \Gamma_3 L & \Gamma_1 L^2 & \Gamma_4 L & (\Gamma_2 - \Omega^2 \beta) L^2 \end{bmatrix} \tag{58}$$

Note that in the above summation, elements of $\mathbf{D}_2(\omega)$ are added with the elements of the matrix $\mathbf{D}(\omega)$ corresponding to the relevant degrees of freedom (3 and 4 in this case).

4.2. The consideration of damped and flexible foundation

The importance of flexibility of foundation is now well recognised [34]. In the previous works by the authors [16,18] it was observed that the first undamped natural frequency of the system is sensitive to the stiffness parameters related to the foundation. The effect of damping in the foundation has never been taken into account in the context of dynamics of wind turbine towers. Here we propose a novel and a simple approach to include the effect of foundation stiffness and damping simultaneously by using the idea of a 'zero-length finite element' corresponding to point 1 in Fig. 1. Three types of stiffness constants [19] and three types of damping constants are used to model damped soil-structure interaction:

(a) Lateral spring and damper k_l and c_l
(b) Rotational spring and damper k_r and c_r
(c) Cross spring and damper k_{lr} and c_{lr}

The dynamic equilibrium for the virtual element corresponding to point 1 in Fig. 1 we have the matrix equation

$$\underbrace{\begin{bmatrix} k_l + \mathrm{i}\omega c_l & -(k_{lr} + \mathrm{i}\omega c_{lr}) \\ -(k_{lr} + \mathrm{i}\omega c_{lr}) & k_r + \mathrm{i}\omega c_r \end{bmatrix}}_{\mathbf{D}_1(\omega)} \begin{Bmatrix} w_1 \\ w_2 \end{Bmatrix} = \begin{Bmatrix} 0 \\ 0 \end{Bmatrix} \tag{59}$$

Following the notations of the degrees of freedom in Fig. 2, it should be noted that w_1 is the displacement and w_1 is the rotation of the bottom point. The forcing vector is considered to be zero as it is assumed that no net external forcing is applied at point 1.

We introduce the following non-dimensional stiffness parameters

$$\eta_l = \frac{k_l L^3}{EI} \quad (\text{nondimensional lateral foundation stiffness}) \tag{60}$$

$$\eta_r = \frac{k_r L}{EI} \quad (\text{nondimensional rotational foundation stiffness}) \tag{61}$$

$$\eta_{rl} = \frac{k_{rl} L^2}{EI} \quad (\text{nondimensional cross foundation stiffness}) \tag{62}$$

Using these, the following new non-dimensional damping parameters are introduced

$$\xi_l = \frac{c_l L}{\eta_l \sqrt{m\, EI}} \quad (\text{lateral foundation damping factor}) \tag{63}$$

$$\xi_r = \frac{c_r}{\eta_r L \sqrt{m\, EI}} \quad (\text{rotational foundation damping factor}) \tag{64}$$

$$\xi_{rl} = \frac{c_{lr}}{\eta_{rl} \sqrt{m\, EI}} \quad (\text{cross foundation damping factor}) \tag{65}$$

In view of these quantities, after some simplifications it can be shown that the dynamic stiffness matrix corresponding to the damped foundation element becomes

$$\mathbf{D}_1(\omega)=\frac{EI}{L^3}\begin{bmatrix}\eta_l(1+\mathrm{i}\Omega\xi_l) & -\eta_{rl}(1+\mathrm{i}\Omega\xi_{rl})L\\ -\eta_{rl}(1+\mathrm{i}\Omega\xi_{rl})L & \eta_r(1+\mathrm{i}\Omega\xi_r)L^2\end{bmatrix} \tag{66}$$

Adding this with the dynamic stiffness matrix of the beam we have the combined stiffness matrix as

$$\mathbf{D}_c(\omega)=\frac{EI}{L^3}\Bigg[\overline{\Gamma}_6\ -\overline{\Gamma}_4L\Gamma_5\Gamma_3L-\overline{\Gamma}_4L\overline{\Gamma}_2L^2-\Gamma_3L\Gamma_1L^2\Gamma_5-\Gamma_3L\big(\Gamma_6 - \Omega^2\overline{\alpha}\big)\Gamma_4L\Gamma_3L\Gamma_1L^2\Gamma_4L\big(\Gamma_2-\Omega^2\overline{\beta}\big)L^2\Bigg] \tag{67}$$

Note that in the above summation, elements of $\mathbf{D}_1(\omega)$ are added with the elements of the matrix $\mathbf{D}_e(\omega)$ corresponding to the relevant degrees of freedom (3 and 4 in this case). Therefore, in the above matrix

$$\overline{\Gamma}_6=\Gamma_6+\eta_l(1+\mathrm{i}\Omega\xi_l) \tag{68}$$

$$\overline{\Gamma}_4=\Gamma_4+\eta_{rl}(1+\mathrm{i}\Omega\xi_{rl}) \tag{69}$$

$$\text{and}\quad \overline{\Gamma}_2=\Gamma_2+\eta_r(1+\mathrm{i}\Omega\xi_r) \tag{70}$$

Equation (67) represents the complete exact and the most general dynamic stiffness matrix corresponding to the damped wind turbine tower model in Fig. 1. The elements of this matrix is given by transcendental function of complex arguments. All the constants necessary to obtain this matrix have been expressed in closed-form using non-dimensional quantities. Next we develop the process of obtaining dynamic response due to selected forcing functions.

5. Dynamic response in the frequency domain

5.1. System with fixed foundation

For systems with a fixed foundation the dynamic stiffness matrix in (58) is used. The complete equilibrium equation is therefore given by

$$\frac{EI}{L^3}\begin{bmatrix}\Gamma_6 & -\Gamma_4L & \Gamma_5 & \Gamma_3L\\ -\Gamma_4L & \Gamma_2L^2 & -\Gamma_3L & \Gamma_1L^2\\ \Gamma_5 & -\Gamma_3L & (\Gamma_6-\Omega^2\overline{\alpha}) & \Gamma_4L\\ \Gamma_3L & \Gamma_1L^2 & \Gamma_4L & (\Gamma_2-\Omega^2\overline{\beta})L^2\end{bmatrix}\begin{Bmatrix}w_1\\ w_2\\ w_3\\ w_4\end{Bmatrix}=\begin{Bmatrix}0\\ 0\\ f_3\\ f_4\end{Bmatrix} \tag{71}$$

Here f_3 and f_4 are amplitudes of the harmonic force and moment applied at the top of the beam. We consider only a transverse force is applied to the top end, therefore, $f_3=F_2$ and $f_4=0$. As $w_1=w_2=0$ due to the fixed end, eliminating first two rows and columns, and using the notation introduced in (27) we obtain

$$\frac{EI}{L^3}\begin{bmatrix}(\Gamma_6-\Omega^2\overline{\alpha}) & \Gamma_4L\\ \Gamma_4L & (\Gamma_2-\Omega^2\overline{\beta})L^2\end{bmatrix}\begin{Bmatrix}\delta^{(2)}(\omega)\\ \theta^{(2)}(\omega)\end{Bmatrix}=\begin{Bmatrix}F_2(\omega)\\ 0\end{Bmatrix} \tag{72}$$

Solving this equation, we obtain the displacement and rotational response corresponding to the top point as

$$\delta^{(2)}(\omega)=\frac{(\Gamma_2-\Omega^2\overline{\beta})}{((\Gamma_6-\Omega^2\overline{\alpha})(\Gamma_2-\Omega^2\overline{\beta})-\Gamma_4^2)}\frac{F_2(\omega)L^3}{EI} \tag{73}$$

$$\theta^{(2)}(\omega)=-\frac{\Gamma_4}{((\Gamma_6-\Omega^2\overline{\alpha})(\Gamma_2-\Omega^2\overline{\beta})-\Gamma_4^2)}\frac{F_2(\omega)L^2}{EI} \tag{74}$$

5.2. System with damped and flexible foundation

For this case the general dynamic stiffness matrix in (67) need to be used. The frequency dependent responses for the four degrees of freedom are obtained by solving the 4×4 system of complex linear equations. The spatial response within the wind turbine tower should be obtained with the complex shape functions as given in (18). We consider two case of forcing. In the first case, only a transverse force acting on the top point is considered. This is similar what discussed in the previous subsection. The forcing vector is given by

$$\mathbf{f}(\omega)=\begin{Bmatrix}f_1(\omega)\\ f_2(\omega)\\ f_3(\omega)\\ f_4(\omega)\end{Bmatrix}=\begin{Bmatrix}0\\ 0\\ F_2(\omega)\\ 0\end{Bmatrix} \tag{75}$$

Solving the equilibrium equation (26) with the general dynamic stiffness matrix in (67), we obtain the displacement response corresponding to the bottom point as

$$\delta^{(1)}(\omega)=\Big\{\Omega^4\overline{\alpha}\overline{\beta}\overline{\Gamma}_2+\Big(\overline{\beta}\Gamma_3^2+(-\overline{\alpha}\Gamma_2-\overline{\beta}\Gamma_6)\overline{\Gamma}_2+\overline{\alpha}\Gamma_1^2\Big)\Omega^2-\Gamma_2\Gamma_3^2-2\,\Gamma_1\Gamma_3\Gamma_4+\overline{\Gamma}_2\big(\Gamma_2\Gamma_6-\Gamma_4^2\big)-\Gamma_1^2\Gamma_6\Big\}\frac{F_2(\omega)L^3}{EI\ \Delta_c} \tag{76}$$

$$\begin{aligned}\Delta_c=&\overline{\alpha}\overline{\beta}\Big(\overline{\Gamma}_2\overline{\Gamma}_6-\overline{\Gamma}_4^2\Big)\Omega^4+\Big(\Big(\overline{\alpha}\overline{\Gamma}_2+\overline{\beta}\overline{\Gamma}_6\Big)\Gamma_3^2+2\,\overline{\Gamma}_4(\overline{\alpha}\Gamma_1-\overline{\beta}\Gamma_5)\Gamma_3\Big)\\ &+\Big(-\overline{\alpha}\overline{\Gamma}_6\Gamma_2-b\Big(-\Gamma_5^2+\Gamma_6\overline{\Gamma}_6\Big)\Big)\overline{\Gamma}_2+\overline{\alpha}\overline{\Gamma}_6\Gamma_1^2+\overline{\Gamma}_4^2(\overline{\alpha}\Gamma_2+\overline{\beta}\Gamma_6)\Omega^2+\Gamma_3^4\\ &+\Big(2\,\Gamma_1\Gamma_5-\overline{\Gamma}_6\Gamma_2-2\,\overline{\Gamma}_4\Gamma_4-\overline{\Gamma}_2\Gamma_6\Big)\Gamma_3^2+\Big(2\,\Gamma_4\Gamma_5\overline{\Gamma}_2+\Big(-2\,\Gamma_4\overline{\Gamma}_6-2\,\Gamma_6\overline{\Gamma}_4\Big)\Gamma_1+2\,\Gamma_2\Gamma_5\overline{\Gamma}_4\Big)\Gamma_3\\ &+\Big(\Big(-\Gamma_5^2+\Gamma_6\overline{\Gamma}_6\Big)\Gamma_2-\Gamma_4^2\overline{\Gamma}_6\Big)\overline{\Gamma}_2+\Big(\Gamma_5^2-\Gamma_6\overline{\Gamma}_6\Big)\Gamma_1^2+2\,\Gamma_1\Gamma_4\Gamma_5\overline{\Gamma}_4-\overline{\Gamma}_4^2\big(\Gamma_2\Gamma_6-\Gamma_4^2\big)\end{aligned} \tag{77}$$

In the above equation, Δ_c, the determinant of the general dynamic stiffness matrix in (67) is given by

The displacement corresponding to the top point is obtained as

$$\delta^{(2)}(\omega) = \left\{\Gamma_3^2\overline{\Gamma}_2 + 2\,\Gamma_1\Gamma_3\overline{\Gamma}_4 + \left(-\Omega^2\overline{\beta} + \Gamma_2\right)\overline{\Gamma}_4^2 + \overline{\Gamma}_6\left(\Omega^2\overline{\beta\Gamma}_2 + \Gamma_1^2 - \Gamma_2\overline{\Gamma}_2\right)\right\}\frac{F_2(\omega)L^3}{EI\,\Delta_c} \tag{78}$$

Next we consider the case when only a transverse force acting on the bottom point. The forcing vector is given by

$$\mathbf{f}(\omega) = \begin{Bmatrix} f_1(\omega) \\ f_2(\omega) \\ f_3(\omega) \\ f_4(\omega) \end{Bmatrix} = \begin{Bmatrix} F_1(\omega) \\ 0 \\ 0 \\ 0 \end{Bmatrix} \tag{79}$$

Solving the equilibrium equation, we obtain the displacement response corresponding to the bottom and top points as

$$\delta^{(1)}(\omega) = \left\{\Omega^4\overline{\alpha\beta\Gamma}_2 + \left(\overline{\beta}\Gamma_3^2 + \left(-\overline{\alpha\Gamma}_2 - \overline{\beta\Gamma}_6\right)\overline{\Gamma}_2 + \overline{\alpha}\Gamma_1^2\right)\Omega^2 - \Gamma_2\Gamma_3^2 - 2\,\Gamma_1\Gamma_3\Gamma_4 + \overline{\Gamma}_2\left(\Gamma_2\Gamma_6 - \Gamma_4^2\right) - \Gamma_1^2\Gamma_6\right\}\frac{F_1(\omega)L^3}{EI\,\Delta_c} \tag{80}$$

and

$$\delta^{(2)}(\omega) = \left\{\Gamma_1\Gamma_3^2 + \left(\left(-\Omega^2\overline{\beta} + \Gamma_2\right)\overline{\Gamma}_4 + \overline{\Gamma}_2\Gamma_4\right)\Gamma_3 + \Gamma_1\Gamma_4\overline{\Gamma}_4 + \Gamma_5\left(\Omega^2\overline{\beta\Gamma}_2 + \Gamma_1^2 - \Gamma_2\overline{\Gamma}_2\right)\right\}\frac{F_1(\omega)L^3}{EI\,\Delta_c} \tag{81}$$

Although closed-form expressions have been obtained in the above expressions, a direct numerical approach can also be employed if necessary.

The method developed here is essentially a frequency domain approach. The response in the time-domain can be obtained using the usual Fourier transform of the frequency domain data. It should be noted that geometric nonlinearity arising due to the compression of the wind turbine tower is already included in the formulation. However, material nonlinearly is not considered in this initial work. Nonlinear behaviour in the stiffness and damping properties can arise due to the interaction with the foundation (soil) and aerodynamics of the turbine blades. From the point of view of this analysis, such nonlinearities will only impact the additional terms added to the dynamic stiffness matrix in (31) and not the dynamic stiffness matrix itself. For weak material nonlinearities, perturbation-based methods [35] can be developed for a more refined dynamic analysis.

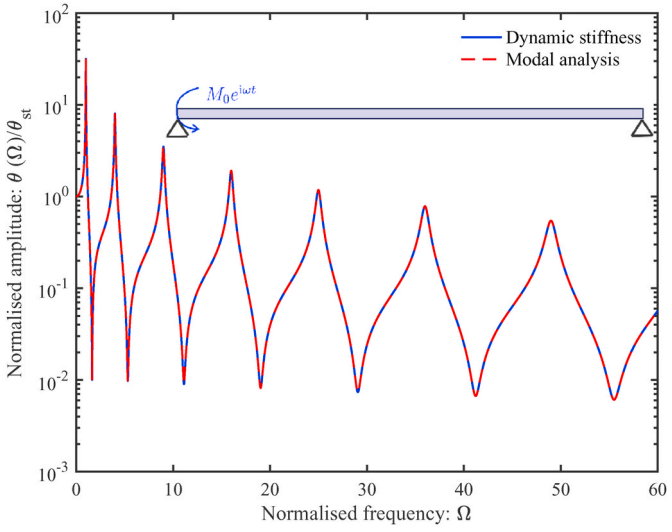

Fig. 3. The amplitude of the normalised rotation at the left end of a pinned-pinned beam due to an applied harmonic moment at the same point. The rotation is normalised with respect to the equivalent static response and plotted as a function of the normalised frequency. The damping factor values are $\xi_2 = 1 \times 10^{-2}$ and $\xi_1 = 0$.

6. Numerical validation and illustration

6.1. Validation with respect to modal analysis

Modal analysis [20] is the classical approach for dynamic response analysis of complex systems. When used in conjunction with the finite element method, the system is divided into a number of elements. Eigenvalues and eigenvectors are then calculated by solving the generalised eigenvalue problem involving the mass and stiffness matrices of the system. The dynamic response is calculated using the superposition of the eigenmodes. We consider a pinned-pinned beam to compare the results from the proposed dynamic stiffness approach with the modal analysis.

Dynamic response due to a harmonic moment at one end as shown in Fig. 3 is considered.

Using the notation introduced in (27) and considering the pinned-pinned boundary condition, eliminating first and third rows and columns of the dynamic stiffness matrix in (31) we obtain

$$\frac{EI}{L^3}\begin{bmatrix} \Gamma_2L^2 & \Gamma_1L^2 \\ \Gamma_1L^2 & \Gamma_2L^2 \end{bmatrix}\begin{Bmatrix} \theta^{(1)}(\omega) \\ \theta^{(2)}(\omega) \end{Bmatrix} = \begin{Bmatrix} M_0(\omega) \\ 0 \end{Bmatrix} \tag{82}$$

Solving this equation, we derive the rotational responses and the two ends as

$$\begin{Bmatrix} \theta^{(1)}(\omega) \\ \theta^{(2)}(\omega) \end{Bmatrix} = \frac{L}{EI(\Gamma_2^2 - \Gamma_1^2)}\begin{Bmatrix} \Gamma_2M_0 \\ -\Gamma_1M_0 \end{Bmatrix} \tag{83}$$

For the special case when the moment is a static moment, considering $\omega \to 0$, from (47) we have $\Gamma_2 \to 4$ and $\Gamma_2 \to 2$. Using this we obtain $\theta^{(1)} = M_0L/3EI$ and $\theta^{(2)} = -M_0L/6EI$. They match exactly with the classical expressions. Hence the dynamic response given by equation (83) is the generalisation of the static response to the damped case in the frequency domain. The amplitude of the normalised rotation at the left end ($\theta^{(1)}$) is shown Fig. 3. For the numerical calculations, $L = 1$ m, $EI/m = 10^4$ and $M_0 = 1$ are used. In the same plot, the result obtained from the classical modal analysis is also shown. The dynamic stiffness method and the modal analysis match exactly. While the dynamic stiffness approach uses only one element, 100 elements were used for the modal analysis. This requires the solution of a general eigenvalue problem with

Table 2
Material and geometric properties of the turbine structure considered for dynamic response analysis.

Turbine Structure Properties	Numerical values
Length (L)	81 m
Average diameter (D)	3.5 m
Thickness (t_h)	0.075 mm
Mass density (ρ)	7800 kg/m^3
Young's modulus (E)	2.1×10^{11} Pa
Mass density (ρ_t)	7800 kg/m^3
Rotational speed (ϖ)	22 r.p.m = 0.37 Hz
Top mass (M)	130,000 kg
Rated power	3 MW

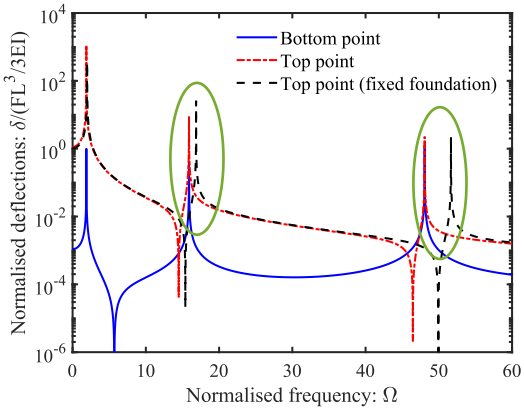

Fig. 4. The amplitude of the normalised lateral deflection at the bottom and top end of the wind turbine due to an applied harmonic force at the top end plotted as functions of the normalised frequency. The displacement is normalised with respect to the equivalent static response. The damping factor values are $\xi_2 = 1 \times 10^{-3}$ and all the others are zero.

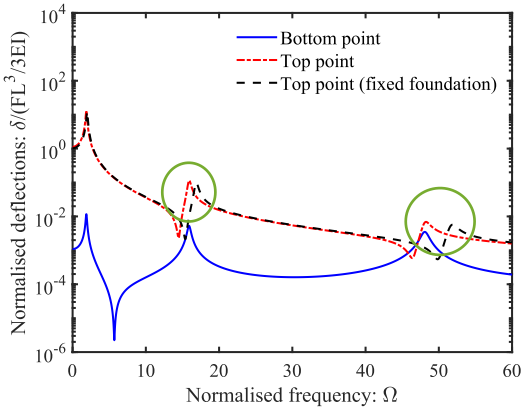

Fig. 5. The amplitude of the normalised lateral deflection at the bottom and top end of the wind turbine due to the applied harmonic excitation at the top end plotted as functions of the normalised frequency. The displacement is normalised with respect to the equivalent static response. The damping factor values are $\xi_M = 1 \times 10^{-1}$, $\xi_J = 1 \times 10^{-2}$ and all the others are zero.

200×200 dimensional matrices. This comparative analysis clearly demonstrates not only the computational efficiency of the dynamic stiffness method but also the fact that the complete damped dynamic response can be obtained using simple closed-form expressions as in equation (83). Next, we apply the proposed approach to a practical wind turbine problem.

6.2. Illustrative example

The analytical formulations derived in the previous sections are presented in terms of non-dimensional parameters. This provides a convenient and general approach to consider dynamic response analysis of wide range of wind turbine structures in a unified manner. In this section we provide numerical illustrations to demonstrate this process.

Example of a wind turbine used in Ref. [16] is employed. The numerical values of the main parameters are summarised in Table 2.

The moment of inertia of the circular cross section can be obtained as

$$I = \frac{\pi}{64}D^4 - \frac{\pi}{64}(D - t_h)^4 \approx \frac{1}{16}\pi D^3 t_h = 0.6314m^4 \tag{84}$$

The mass density per unit length of the system can be obtained as

$$m = \rho A \approx \rho \pi D t_h/2 = 3.1817 \times 10^3 \text{kg/m} \tag{85}$$

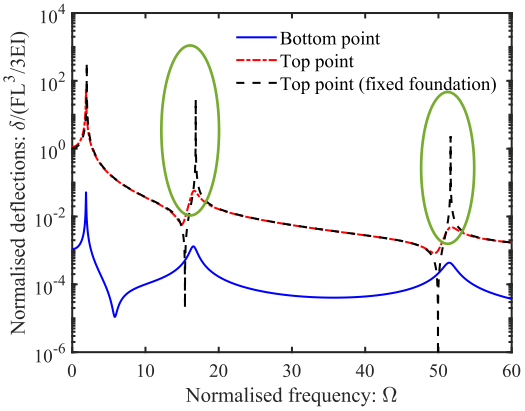

Fig. 6. The amplitude of the normalised lateral deflection at the bottom and top end of the wind turbine due to the applied harmonic excitation at the top end plotted as functions of the normalised frequency. The displacement is normalised with respect to the equivalent static response. The damping factor values are $\xi_l = 1 \times 10^{-1}$, $\xi_r = 1 \times 10^{-1}$, $\xi_{lr} = 1 \times 10^{-1}$ and all the others are zero.

Table 3
Physics-based damping factors necessary for the dynamic analysis of wind turbines.

Damping category	Damping factor	Notation	Analytical formula	Suggested values
A: Wind turbine tower damping	Strain-rate-dependent damping factor	ξ_1	$\frac{c_1}{L^2\sqrt{m\,EI}}$	10^{-3} - 10^{-5}
	Velocity-dependent damping factor	ξ_2	$\frac{c_2 L^2}{\sqrt{m\,EI}}$	10^{-2} - 10^{-3}
B: Foundation/soil damping	Lateral foundation damping factor	ξ_l	$\frac{c_l L}{\eta_l\sqrt{m\,EI}}$	10^{-1} - 10^{-2}
	Rotational foundation damping factor	ξ_r	$\frac{c_r}{\eta_r L\sqrt{m\,EI}}$	10^{-2} - 10^{-3}
	Cross foundation damping factor	ξ_{lr}	$\frac{c_{lr}}{\eta_{rl}\sqrt{m\,EI}}$	10^{-1} - 10^{-4}
C: Damping corresponding to the nacelle	Aerodynamic mass damping factor	ξ_M	$\frac{c_M L}{\sqrt{m\,EI}}$	10^{-1} - 10^{-3}
	Aerodynamic rotary damping factor	ξ_J	$\frac{c_J}{L\sqrt{m\,EI}}$	10^{-2} - 10^{-4}

Using these, the mass ratio $\alpha = 00.5044$ and the nondimensional axial force $\nu = 0.0652$. The rotary inertia parameter β is assumed to be zero. We also obtain the natural frequency scaling parameter as

$$c_0 = \frac{EI}{mL^4} = 0.9682 \text{ s}^{-1} \tag{86}$$

The radius of gyration of the wind turbine is given by

$$r = \sqrt{\frac{I}{A}} = \frac{1}{4}\sqrt{D^2 + (D - t_h)^2} \approx \frac{D}{2\sqrt{2}} = 1.2374m \tag{87}$$

Therefore, the nondimensional radius of gyration $\mu = r/L = 0.0151$. From Eq. (7) we therefore have

$$\widetilde{\nu} = \nu + 2.2844 \times 10^{-4}\Omega^2 \approx \nu \tag{88}$$

The non-dimensional parameters corresponding to the foundation stiffness are given by $\eta_l = 3000, \eta_r = 30, \eta_{rl} = -60$. Details of the natural frequency analysis can be found in Ref. [16].

Here we focus on the dynamic response calculations. For this, the key additional parameters necessary are the seven damping parameters

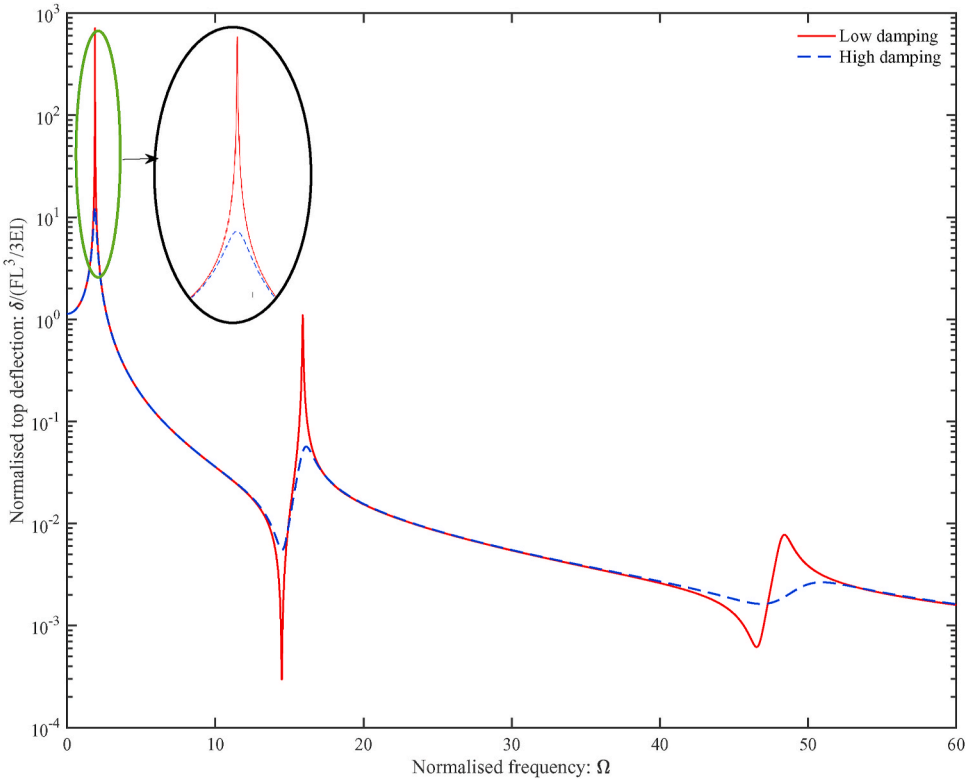

Fig. 7. The amplitude of the normalised lateral deflection at the top end of the wind turbine due to an applied harmonic force at the top end plotted as a function of the normalised frequency. The two cases shown correspond to low and high values of the damping factors given in Table 3.

introduced in the paper. We consider three cases of damping parameters. In the first case, only the tower is damped. In the second case, we consider only the aerodynamic damping at the nacelle of the wind turbine. The last case is when damping is present only at the foundation. These cases are considered to understand and differentiate the impact of different damping parameters. In Fig. 4 we show the amplitude of the normalised lateral deflection at the bottom and top end of the wind turbine due to an applied harmonic force at the top end.

The response at the bottom point is significantly smaller compared to the response at the top point as expected. The peaks in the response correspond to the natural frequencies of the system. There are three natural frequencies within the frequency range considered. In the same plot, the response at the top end when the foundation is fixed (like a cantilever) is also shown. This system is stiffer as it shows higher natural frequencies compared to wind turbine with a flexible foundation. The difference between the two case increase in hinger frequencies (marked in Fig. 4).

The amplitude of the normalised lateral deflections are shown in Fig. 5 when only the aerodynamic damping at the nacelle of the wind turbine is considered.

This case demonstrates a considerable damped response to the wind turbine. The response at top point (where the dampers are) diminishes sharply at higher frequencies to an extent that it almost matches with that at the bottom point (marked in Fig. 5).

In Fig. 6, the amplitude of the normalised lateral deflections are shown when damping is present only at the foundation.

We can see orders of magnitude difference in response between the case of the fixed and the flexible foundation case (marked in Fig. 6). This is arising because the tower with the fixed foundation is effectively undamped and therefore has a very high response around the resonance frequencies. This plot also demonstrates that the dynamic response of the wind turbine can be controlled with properly designed dampers at the foundation.

Explicit consideration of physics-based damping factors is a key novel feature of the proposed approach. All the seven crucial damping factors identified here are summarised in Table 3.

Some suggested values of the damping factors are given in the table. To understand the effects of different damping factors we consider two extreme cases comprising of lower and higher values given in the table. In Fig. 7 The amplitude of the normalised lateral deflection at the top end of the wind turbine due to an applied harmonic force at the top end is shown for low and high values of the damping factors given in Table 3.

It can be observed that a significant difference in the dynamic response, particular in the first mode, can occur due to the difference in the damping factors values. The method developed in this paper can comprehensively incorporate different physics-based damping factors in a unified manner. This presents a platform for analysing and understanding the impact of damping factors on the dynamic design of wind turbines.

7. Conclusion

The quantification of the dynamic response of wind turbine towers due to various external forces is of paramount importance. A physics-based analytical approach leading to closed-form expressions of essential dynamic response quantities was presented. The route to this analytical derivation has three key steps. Firstly, noting that the wind turbine tower is a beam-like structure, the dynamic stiffness matrix of a beam with axial compressive force is derived exactly. This is achieved using transcendental displacement functions which are exact solutions of the governing partial differential equation with appropriate boundary conditions. Due to the presence of damping, the elements of the dynamic stiffness coefficients are complex-valued functions of the frequency. Secondly, to take account of the foundation stiffness and damping, the mass and rotary inertia of the nacelle along with aerodynamic damping, additional elements are added to the pristine dynamic stiffness matrix derived in the first step. Finally, resulting compound dynamic stiffness is inverted with appropriate boundary conditions to obtain the dynamic

response through closed-form expressions. These expressions are exact and valid for any frequency of the applied forcing. Direct comparison with modal analysis confirms that the proposed dynamic stiffness approach produces the same results. However, unlike the classical modal analysis, the determination of natural frequencies and mode shapes are not necessary and only one element is sufficient to obtain the dynamic response across the frequency ranges.

The analytical results derived in the paper are in terms of several non-dimensional parameters. This makes them general and applicable to any wind turbine structures. As the method is essentially a frequency domain approach, it is straightforward to obtain the output spectral function from any given input spectral function of the applied forcing. A key novel feature is the introduction of seven physically-based damping factors. They have been classed into three distinct groups, (a) velocity and strain-dependent damping factors of the wind turbine tower, (b) mass and rotary damping factors of the nacelle, and (c) lateral, rotational and cross damping factors of the foundation. This approach enables a more precise route to the damping quantification which is important not only for the response-amplitude determination but also for long-term fatigue prediction. It is not possible to incorporate damping in this physical manner using the conventional modal approach. Limited numerical results shown in the paper clearly demonstrate in the impact of different damping groups on the dynamic response due to harmonic excitation. The numerical analysis also shows how the dynamic response in the higher modes can be obtained simply using the formulae given in the paper. Future research is needed towards the experimental determination of the seven new damping factors introduced here.

Author statement

The two authors have equal contribution to the paper.

Declaration of competing interest

The authors declare that they have no known competing financial interests or personal relationships that could have appeared to influence the work reported in this paper.

References

[1] Arany L, Bhattacharya S. Simplified load estimation and sizing of suction anchors for spar buoy type floating offshore wind turbines. Ocean Eng 2018;159:348–57.
[2] De Risi R, Bhattacharya S, Goda K. Seismic performance assessment of monopile-supported offshore wind turbines using unscaled natural earthquake records. Soil Dynam Earthq Eng 2018;109:154–72.
[3] S. Bhattacharya, Design of foundations for offshore wind turbines, Wiley Online Library.
[4] Adedipe O, Brennan F, Kolios A. Corrosion fatigue load frequency sensitivity analysis. Mar Struct 2015;42:115–36.
[5] Chortis G, Askarinejad A, Prendergast L, Li Q, Gavin K. Influence of scour depth and type on p–y curves for monopiles in sand under monotonic lateral loading in a geotechnical centrifuge. Ocean Eng 2020:106838.
[6] Zuo H, Bi K, Hao H. Using multiple tuned mass dampers to control offshore wind turbine vibrations under multiple hazards. Eng Struct 2017;141:303–15.
[7] Sellami T, Berriri H, Darcherif AM, Jelassi S, Mimouni MF. Modal and harmonic analysis of three-dimensional wind turbine models. Wind Eng 2016;40(6):518–27.
[8] Banerjee A, Chakraborty T, Matsagar V. Stochastic dynamic analysis of an offshore wind turbine considering frequency-dependent soil–structure interaction parameters. Int J Struct Stabil Dynam 2018;18:1850086. 06.
[9] P. D. Sclavounos, Y. Zhang, Y. Ma, D. F. Larson, Offshore wind turbine nonlinear wave loads and their statistics, J Offshore Mech Arctic Eng 141 (3).
[10] Q. Wang, Z. Wang, B. Fan, Coupled bending and torsional vibration characteristics analysis of inhomogeneous wind turbine tower with variable cross section under elastic constraint, Appl Math Model.
[11] Júnior CVC, de Alencar Araújo RC, de Souza CMC, Ferreira ACA, Ribeiro PMV. A collocation method for bending, torsional and axial vibrations of offshore wind turbines on monopile foundations. Ocean Eng 2020;217:107735.
[12] He R, Kaynia AM, Zhang J, Chen W. Seismic response of monopiles to vertical excitation in offshore engineering. Ocean Eng 2020;216:108120.
[13] Patra SK, Haldar S. Fore-aft and the side-to-side response of monopile supported offshore wind turbine in liquefiable soil. Mar Georesour Geotechnol 2020:1–22.
[14] Zhao M, Gao Z, Wang P, Du X. Response spectrum method for seismic analysis of monopile offshore wind turbine. Soil Dynam Earthq Eng 2020;136:106212.
[15] Jiang W, Lin C, Sun M. Seismic responses of monopile-supported offshore wind turbines in soft clays under scoured conditions. Soil Dynam Earthq Eng 2021;142:106549.
[16] Adhikari S, Bhattacharya S. Dynamic analysis of wind turbine towers on flexible foundations. Shock Vib 2012;19(1):37–56.
[17] Adhikari S, Bhattacharya S. Vibrations of wind-turbines considering soil-structure interaction, Wind and Structures. Int J 2011;14(2):85–112.
[18] Bhattacharya S, Adhikari S. Experimental validation of soil-structure interaction of offshore wind turbines. Soil Dynam Earthq Eng 2011;31(4–6):805–16.
[19] Arany L, Bhattacharya S, Adhikari S, Hogan SJ, Macdonald J. An analytical model to predict the natural frequency of offshore wind turbines on three-spring flexible foundations using two different beam models. Soil Dynam Earthq Eng 2015;74(1):40–5.
[20] Meirovitch L. Principles and techniques of vibrations. New Jersey: Prentice-Hall International, Inc.; 1997.
[21] Paz M. Structural dynamics: theory and computation. second ed. Reinhold: Van Nostrand; 1980.
[22] Leung AYT. Dynamic stiffness and substructures. London, UK: Springer-Verlag; 1993.
[23] Manohar CS, Adhikari S. Dynamic stiffness of randomly parametered beams. Probabilist Eng Mech 1998;13(1):39–51.
[24] Banerjee JR. Dynamic stiffness formulation for structural elements: a general approach. Comput Struct 1997;63(1):101–3.
[25] Adhikari S, Manohar CS. Transient dynamics of stochastically parametered beams. ASCE J. Eng. Mech. 2000;126(11):1131–40.
[26] Doyle JF. Wave propagation in structures. New York: Springer Verlag; 1989.
[27] Adhikari S, Murmu T, McCarthy M. Dynamic finite element analysis of axially vibrating nonlocal rods. Finite Elem Anal Des 2013;63(1):42–50.
[28] Liu X, Banerjee J. A spectral dynamic stiffness method for free vibration analysis of plane elastodynamic problems. Mech Syst Signal Process 2017;87:136–60.
[29] Adhikari S, Karlicic D, Liu X. Dynamic stiffness method for nonlocal damped nano-beams on elastic foundation. Eur J Mech Solid 2021;86(3–4):104144.
[30] Inman DJ. Engineering vibration. NJ, USA: Prentice Hall PTR; 2003.
[31] Géradin M, Rixen D. Mechanical vibrations. second ed. New York, NY: John Wiely & Sons; 1997. translation of: Théorie des Vibrations.
[32] Petyt M. Introduction to finite element vibration analysis. Cambridge, UK: Cambridge University Press; 1998.
[33] Dawe D. Matrix and finite element displacement analysis of structures. Oxford, UK: Oxford University Press; 1984.
[34] Bisoi S, Haldar S. Dynamic analysis of offshore wind turbine in clay considering soil–monopile–tower interaction. Soil Dynam Earthq Eng 2014;63:19–35.
[35] Nayfeh AH, Mook DT. Nonlinear oscillations. New York, NY: John Wiely & Sons; 1979.